Why does *Trichodesmium* become abundant in the Kuroshio?

T. Shiozaki[1,2], S. Takeda[1,3], S. Itoh[2], T. Kodama[1,4], X. Liu[1,5], F. Hashihama[6], K. Furuya[1]

[1]{Department of Aquatic Bioscience, Graduate School of Agricultural and Life Sciences, The University of Tokyo, Tokyo, 113-8657, Japan}

[2]{Atmosphere and Ocean Research Institute, The University of Tokyo, Chiba, 277-8564, Japan}

[3]{Faculty of Fisheries, Nagasaki University, Nagasaki, 852-8521, Japan}

[4]{Japan Sea National Fisheries Research Institute, Fisheries Research Agency, Niigata, 951-8121, Japan}

[5]{College of Ocean and Earth Sciences, Xiamen University, Xiamen, 361005, China}

[6]{Department of Ocean Sciences, Tokyo University of Marine Science and Technology, Tokyo, 108-8477, Japan}

Corresponding to: T. Shiozaki (shiozaki@aori.u-tokyo.ac.jp)

Abstract

The genus *Trichodesmium* is recognized as abundant and major diazotroph in the Kuroshio, but the reason for this remains unclear. The present study investigated the abundance of *Trichodesmium* spp. and nitrogen fixation together with concentrations of dissolved iron and phosphate in the Kuroshio and its marginal seas. We performed the observations near the Miyako Islands, which form part of the Ryukyu Islands, situated along the Kuroshio, since our satellite analysis suggested that material transport could occur from the islands to the Kuroshio. *Trichodesmium* spp. bloomed (>20,000 filaments L^{-1}) near the Miyako Islands, abundance was high in the Kuroshio and the Kuroshio bifurcation region of the East China Sea, but was low in the Philippine Sea. The abundance of *Trichodesmium* spp. was significantly correlated with the total nitrogen fixation activity. The surface concentrations of dissolved iron (0.19–0.89 nM) and phosphate (<3–36 nM) were similar for all of the study areas, indicating that the nutrient distribution could not explain the spatial differences in *Trichodesmium* spp. abundance and nitrogen fixation. Numerical particle-tracking experiments simulated the transportation of water around the Ryukyu Islands to the Kuroshio. Our results indicate that *Trichodesmium* growing around the Ryukyu Islands could be advected into the Kuroshio.

1. Introduction

The Kuroshio is a western boundary current in the North Pacific Ocean that originates in the North Equatorial Current and bifurcates to the east of the Philippines. The main stream of the Kuroshio enters the East China Sea (ECS) northeast of Taiwan, flows out through the Tokara Strait, and runs along the Japanese islands of Shikoku and Honshu. While the Kuroshio and its adjacent waters are characterized by highly oligotrophic condition, phytoplankton and zooplankton communities in the Kuroshio are distinct compared to those from adjacent waters (McGowan, 1971). McGowan (1971) suggested that some plankton species are delivered by the Kuroshio to the north from the equatorial region.

The abundance of the cyanobacterial genus *Trichodesmium* in the Kuroshio is much higher than that in neighboring seas (Marumo and Asaoka, 1974). Because *Trichodesmium* is a major nitrogen fixer in the Kuroshio, it is believed to be the key genus for understanding the Kuroshio ecosystem (Chen et al., 2008, 2014; Shiozaki et al., 2014a). Nevertheless, the factors controlling the distribution of *Trichodesmium* in this region are poorly understood. Marine nitrogen fixation is generally regulated by the supply of iron and phosphorus (Mahaffey et al., 2005), and *Trichodesmium* thrives in iron-rich oligotrophic regions (Moore et al., 2009; Shiozaki et al., 2010, 2014b). A

major source of iron in the ocean is atmospheric dust deposition (Jickells et al., 2005; Mahowald et al., 2009). Modeling studies indicate that dust deposition in the western North Pacific decreases exponentially from the continental shelf to the Philippine Sea (Jickells et al., 2005; Mahowald et al., 2009), and hence, deposition is not as high in the Kuroshio as in the adjacent waters. As for phosphorus limitation, iron-enhanced nitrogen fixation causes phosphorus depletion, and is consequently limited by phosphorus (Mather et al., 2008). The phosphate distribution has been examined in this study region using a conventional colorimetric method, and the surface phosphate concentration in the Kuroshio has been reported to be as low as that in the Philippine Sea (Chen, 2008). Therefore, the distinct high abundance of *Trichodesmium* in the Kuroshio is probably not explained by nutrient condition; however, distributions of dissolved iron and phosphate at nanomolar level have not been well studied in this region (Obata et al., 1997; Shiozaki et al., 2010; Kodama et al., 2011).

Nitrogen fixation by *Trichodesmium* has recently also been found to be active around oceanic islands (Shiozaki et al., 2010, 2013, 2014c). Furthermore, these studies demonstrated that abundant *Trichodesmium* is delivered by the current to areas that are remote from the islands. Although this phenomenon was noted in the western Pacific warm pool and western South Pacific, it can also occur in and around the

73 Kuroshio and may contribute to the distribution of *Trichodesmium* in this region.

74 In the present study, we simultaneously determined *Trichodesmium* abundance
75 and bulk water nitrogen fixation together with concentrations of dissolved iron and
76 phosphate at the nanomolar level in the Kuroshio and its marginal seas. In addition,
77 we conducted intensive observations around the Miyako Islands section of the
78 Ryukyu Islands located close to the main stream of the Kuroshio.

79

80 2. Materials and Methods

81 2.1. Oceanographic database

82 Algal blooms in an oligotrophic region may indicate a nitrogen fixation hotspot
83 (Wilson and Qiu, 2008; Shiozaki et al., 2014c). To identify the locations of intensive
84 algal blooms, we used a dataset of chlorophyll (chl) *a* observed by satellite.
85 According to Wilson and Qiu (2008), an algal bloom in an oligotrophic region can be
86 defined as a chl *a* value >0.15 mg m^{-3} in summer. In the present study, we used 8-day,
87 moderate-resolution imaging spectroradiometer (MODIS) level 3 chl *a* with 9 km
88 resolution during summer between July 2003 and September 2009. We defined as
89 summer July through September. The bloom frequency for each pixel was calculated
90 from the ratio of counts in which chl *a* was >0.15 mg m^{-3} to the total counts in which

91 chl *a* was detected.

92 To examine the current field, geoelectrokinetograph and ship-mounted acoustic
93 Doppler current profiler (ADCP) data from the uppermost layer for the summers
94 between 1953 and 2008 were obtained from the Japan Oceanographic Data Center
95 (http://www.jodc.go.jp). Regridding, removal of anomalous values, and smoothing of
96 the dataset were performed as described by Isobe (2008).

97

98 ## 2.2. **Cruise observations**

99 Experiments were conducted during summer on-board the R/V *Tansei-maru*
100 (KT-06-21, September 9–17, 2006; KT-07-22, September 5–13, 2007; KT-09-17,
101 September 8–13, 2009; KT-10-19, September 4–12, 2010) and the T/V
102 *Nagasaki-maru* (242, July 19–28, 2007) (Fig. 1a, Table S1). The stations during the
103 KT-06-21, KT-07-22, and *Nagasaki-maru* 242 cruises were divided into three areas
104 based on the temperature-salinity diagram (see Fig.2 of Shiozaki et al., 2011): the
105 ECS, Kuroshio, and Philippine Sea. During the KT-09-17 cruise, we conducted
106 experiments around the Miyako Islands which were distinguished from the other three
107 areas. During the KT-10-19 cruise, we performed observations in the ECS, the
108 Kuroshio, and around the Miyako Islands (Liu et al., 2013).

109

110 ### 2.2.1. **Light intensity, hydrography, nutrients, and chl *a***

111 Water samples for all of the experiments, with the exception of determination of
112 the dissolved iron concentration, were collected using an acid-cleaned bucket and
113 Niskin-X bottles. The depth profile of light intensity was determined immediately
114 before the water sampling using a light sensor (during the KT-06-22, KT-07-21,
115 KT-09-17, and KT-10-19 cruises) or an empirical equation (during the
116 *Nagasaki-maru* 242 cruise) (Shiozaki et al., 2011). Temperature and salinity profiles
117 to a depth of 200 m were obtained using a conductivity, temperature, and depth
118 (CTD) sensor. Mixed layer depth (MLD) was defined as the depth at which the
119 sigma-t increased by 0.125 from its value at a depth of 10 m. Water samples for
120 nitrate+nitrite (N+N) and phosphate were collected from 0, 10, 30, 40, 50, 60, 70, 80,
121 90, 100, 125, 150, and 200 m, and from depths at given light intensities. At all of the
122 stations, the N+N and phosphate concentrations were determined at the nanomolar
123 level using a supersensitive colorimetric system consisting of an AutoAnalyzer II
124 (Technicon) and Liquid Waveguide Capillary Cells (World Precision Instruments,
125 USA) (Hashihama et al., 2009). The detection limits of N+N and phosphate were both
126 3 nM. When the concentration was greater than 0.1 μM, it was determined by

conventional methods using a TRAACS 2000 autoanalyzer (Bran:Luebbe, UK). In addition to the observations at the stations, temperature, salinity, and the *in vivo* chl fluorescence of the surface water were monitored continuously during the cruises by a thermosalinograph (Ocean Seven, Idronaut, Italy) and a fluorometer (Minitracka, Chelsea, UK).

2.2.2. **Dissolved iron**

Water was sampled to estimate the dissolved iron concentration from 0.5-m depth during the KT-06-21 and KT-07-22 cruises and from 10-m depth during the KT-09-17 cruise using an acid-cleaned Teflon bellows pump (AstiPure PFD2; Saint-Gobain) with Teflon tubing (inner diameter = 12 mm). The water was filtered through an acid-cleaned 0.22 μm pore filter (Millipak100; Millipore) connected to the in-line of the Teflon tubing with a Teflon connector. Filtered seawater was collected in a 125 mL low-density polyethylene (LDPE) bottle (Nalgene, Nalge Nunc International), which had been washed using following technique: the sample bottles were sequentially cleaned by soaking in 5% alkali detergent for at least 2 days, in 4 N HCl for at least 1 day, in 0.3 N metal analysis-grade HNO_3 at 60°C overnight, and finally, in Milli-Q water at 60°C overnight. After rinsing with Milli-Q water, the bottles were

145 dried in a laminar flow space and stored in double plastic bags. The filtrate samples
146 were acidified to a pH <1.7 with trace-metal-grade HCl (Tamapure AA-100; Tama
147 Chemicals) in a Class-100 clean-air bench, and stored at room temperature for more
148 than 1 year.

149 The dissolved iron concentration was determined using an automatic Fe(III) flow
150 injection analytical system (Kimoto Electric Co., Ltd.) using a chelating resin
151 pre-concentration and chemiluminescence detection method (Obata et al., 1993). A
152 buffer solution of 10 M formic acid and 2.4 M ammonium formate was added to the
153 samples. The sample pH was adjusted to 3.0 with 20% ammonium hydroxide
154 (NH_4OH; Tamapure AA-10; Tama Chemicals) immediately prior to analysis. The
155 detection limit of this method was 0.05 nM. The SAFe reference standards S1 and D2
156 were measured during the course of sample analysis, and the results were within the
157 range of the published consensus values: S1 = 0.097 ± 0.043 nM and D2 = 0.91 ±
158 0.17 nM (Johnson et al., 2007).

159

160 ### 2.2.3. **Nitrogen fixation and abundance of *Trichodesmium* spp.**

161 Samples for the incubation experiments were collected vertically at all of the
162 stations, except at Sts. T0621, GN-3, and T0905, where samples were only collected

163 from the surface. All samples were collected in duplicate in acid-cleaned 4.5-L
164 polycarbonate bottles. During the *Nagasaki-maru* 242 cruise, water samples were
165 collected from four different depths corresponding to 100%, 25%, 10%, and 1% of the
166 surface light intensity. During the other cruises, samples were collected from a depth
167 of 50% surface light intensity. Samples at 100% surface light intensity were collected
168 from 0 m during all of the cruises, except during the KT-10-19 cruise in which the
169 samples were collected from a depth of 5 m. The bulk water nitrogen fixation activity
170 was determined based on primary production using a dual isotopic ($^{15}N_2$ and ^{13}C)
171 technique (Shiozaki et al., 2009). After ^{13}C-labeled sodium bicarbonate (99 atom%
172 ^{13}C; Cambridge Isotope Laboratories) was added to each bottle, 2 mL of $^{15}N_2$ gas (98
173 + atom% ^{15}N; SI Science Co. Japan) was injected directly into the incubation bottles
174 through a septum using a gastight syringe. The bottles were covered with
175 neutral-density screens to adjust the light level and incubated for 24 h in an on-deck
176 incubator cooled by flowing surface seawater for 24 h. We determined the nitrogen
177 fixation activity using the $^{15}N_2$ gas bubble addition method (Montoya et al., 1996).
178 This method is believed to underestimate the nitrogen fixation rate relative to the $^{15}N_2$
179 gas dissolution method (Mohr et al., 2010). The start time of incubation in this study
180 varied at each station (Table S1). Considering daily periodicity of nitrogen fixation in

each diazotroph (Zehr, 2011) and the time to reach equilibration of the $^{15}N_2$ gas bubble with seawater (>12 h, Mohr et al., 2010), the level of underestimation could vary at each station. Meanwhile, the level of underestimation is known to be low in *Trichodesmium* dominant water because *Trichodesmium* can float to the top of the bottle and directly use the added $^{15}N_2$ in the bubble method (Großkopf et al., 2012). Although the bias of underestimation could not be estimated from the results in this study, the actual nitrogen fixation rate would be higher than the obtained rate.

A recent study demonstrated that commercial $^{15}N_2$ gas could be contaminated by ^{15}N-labeled nitrate and ammonium (Dabundo et al., 2014). We tested the contamination in $^{15}N_2$ gas produced by SI Science Co., Ltd., which was used (from different batch numbers) in the present study (see Supporting Information). Briefly, the $^{15}N_2$ gas was dissolved in aged subtropical surface water, and concentrations of nitrate, nitrite, and ammonium at the nanomolar levels were determined using supersensitive colorimetric systems. The results showed that there were no significant differences between the control and samples to which $^{15}N_2$ had been added (Fig. S1), suggesting that the contamination of nitrate, nitrite, and ammonium in the $^{15}N_2$ gas was insignificant (Supporting Information).

Water samples were collected for microscopic analysis at all light depths during

199 the *Nagasaki-maru* 242 and KT-07-21 cruises, and only from the surface during the
200 KT-06-22, KT-09-17, and KT-10-19 cruises. The samples were fixed using acidified
201 Lugol's solution. *Trichodesmium* spp. were counted using the Utermöhl method under
202 inverted microscope observation. *Trichodesmium* greater than ca. 300 μm in length
203 were counted as 1 filament and shorter lengths were counted as 0.5 filaments. In
204 addition, phytoplankton other than *Trichodesmium* spp. were identified from the
205 samples obtained during the KT-09-17 cruise.
206

207 ## 2.3. **Statistical analysis of environmental variables**

208 We used non-metric multi-dimensional scaling (nMDS) to investigate the spatial
209 differences in the environmental variables that could influence *Trichodesmium* growth
210 and bulk water nitrogen fixation; temperature, mixed layer depth, nitrate, dissolved
211 iron, and phosphate. The environmental variables were transformed by $\log_{10}(x + 1)$
212 prior to analysis. A dissimilarity/similarity matrix between stations was constructed
213 using the Bray-Curtis index. The nMDS was used to visualize similarities in the
214 environmental variables among the stations. An Analysis of Similarity (ANOSIM)
215 was used to test the differences in the environmental variables among the stations.
216

2.4. **Numerical experiments**

Numerical particle-tracking experiments were conducted to investigate the transport of water masses at the surface from areas around the Miyako Islands in the summer season from 2003 to 2009. Surface velocity data were derived from the FRA-JCOPE2 reanalysis product (Miyazawa et al., 2009), which is an eddy-resolving (1/12°) ocean model combined with three-dimensional variational data assimilation (satellites, ARGO floats, and shipboard observations), and is one of the most reliable models for the region around Japan for the above time period. The method of tracking particles was basically the same as in Itoh et al. (2009), but we did not include the random walk for simplicity. The release points of particles were selected at the surface of the model grid points around the coastal waters of the Miyako Islands. We assumed that the particles did not increase, die, or sink from the surface during the experiments. To focus on transport during the summer season (July–September), particles were released one month before the summer (June 1) and were tracked until September 30.

To examine differences in the output depending on the start time within the same year, we also performed experiments starting on June 1, 11, and 21, and July 1 in 2009. The ratio of particles that reached areas downstream of the Tokara Strait

235 (hereafter Area K) (Fig. 7), including the particles' entrainment to the Kuroshio, to
236 total particles released from the Miyako Islands was computed in all experiments. It
237 should be noted that these experiments contained the following two uncertainties.
238 First, the distribution of *Trichodesmium* around the islands, which strongly influences
239 the destinations of particles, was not able to be determined in advance.
240 *Trichodesmium* is known to aggregate and not to occur uniformly in the ocean
241 (Capone et al., 1997). Second, the model cannot reproduce the current very close to
242 the islands. If a water mass very near the islands was delivered to the open ocean by
243 tide and/or river plumes that were not considered in the model, seaward dispersion of
244 particles was likely underestimated.
245

246 ## 3. RESULTS

247 ### 3.1. The Kuroshio path and bloom frequency

248 The average surface current field indicated that the main stream of the Kuroshio
249 flowed along the continental shelf in the ECS, and then passed to the south of the
250 Kyushu and Shikoku Islands (Fig. 1b). In addition, the Kuroshio branch bifurcated
251 northward at 25°N and 30°N at the continental shelf. Hence, all of the stations in the
252 ECS were subject to the influence of the Kuroshio. While the northeastward stream of

253 the Kuroshio was prominent in this region, smaller-scale flows and circulations were
254 observed in the areas around and to the southeast of the Ryukyu Islands. In the west
255 of the main stream of the Kuroshio, because the average chl *a* was over 0.15 mg m^{-3}
256 (Fig. S2), the frequency of chl *a* values >0.15 mg m^{-3} was high (Fig. 1b). In contrast,
257 the bloom frequency in the east of the main stream of the Kuroshio differed from the
258 distribution of the average chl *a*; algal blooms occurred frequently in the Ryukyu
259 Islands. Around the Miyako Islands, water of high bloom frequency was located to
260 the west of the islands, extending to the north.
261
262 ### 3.2. Region-wide environmental conditions, *Trichodesmium* spp., and
263 nitrogen fixation
264 The sea surface temperature (SST) ranged from 25.1–30.5°C at all of the stations
265 (Table S1), and there were no significant differences among the areas (p>0.05,
266 Tukey's honestly significant difference [HSD] test). The MLD varied from 12–60 m
267 at all of the stations, and was relatively deep around the Miyako Islands compared to
268 the other areas (Table S1). The surface N+N concentration varied between <3 and 42
269 nM, except around the Miyako Islands (Shiozaki et al., 2010, 2011) (Table S1). The
270 highest surface N+N concentration (374 nM) was observed at St. T0904 where

upwelling occurred (see below). No significant difference in the surface N+N was observed among the four areas (p>0.05, Tukey's HSD test). The surface phosphate concentration varied between <3 and 36 nM at all of the stations (Fig. 2a). The phosphate concentration at the surface and within the MLD was not significantly different among the four areas (p>0.05, Tukey's HSD test). There was a greater increase in the phosphate concentrations below 40–50 m in the ECS compared to the other areas (Fig. 3a–d). Furthermore, the phosphate concentrations below 40–50 m near the Miyako Islands were higher than those in the Kuroshio and the Philippine Sea, which were depleted down to 100 m, except at St. T1004 located near the continental shelf. The N/P (= N+N/phosphate) ratio at the surface varied from 0.28 to 6.40 except at St. T0904 (N/P = 16.3) (Table S1), and no significant differences were observed among the four areas (p > 0.05, Tukey's HSD test). The surface dissolved iron concentration ranged from 0.19 to 0.89 nM at all of the stations (Fig 2b), with no significant spatial differences among the four areas (p>0.05, Tukey's HSD test). The surface dissolved iron concentration at Sts. T0622 and T0907 was elevated to 0.83 nM and 0.89 nM, respectively, with lower salinity water than in the adjacent waters (salinity data are shown in Fig. 4a and Kodama et al., 2011). The nMDS showed that the environmental variables at all stations were the same at the >80% similarity level

289 and were >90 % similar excepting station T0904 (Fig. 5). The ANOSIM indicated no
290 significant differences among the stations ($p > 0.05$).
291 The abundance of *Trichodesmium* spp. was highest at the surface at almost all of
292 the stations during the *Nagasaki-maru* 242 and KT-07-21 cruises (Fig. S3). The
293 surface *Trichodesmium* spp. abundances were positively correlated with the
294 depth-integrated abundances ($p < 0.05$, *t*-test) (Fig. 6a). Thus, the surface abundance
295 was used to discuss the geographical distribution of *Trichodesmium* spp. The
296 *Trichodesmium* spp. abundance at the surface varied widely, and there was no
297 significant difference among the four areas ($p > 0.05$, Tukey's HSD test).
298 *Trichodesmium* spp. were observed at all of the stations in the Kuroshio and around
299 the Miyako Islands, whereas they were not always observed in the ECS and the
300 Philippine Sea (Fig. 2c). The average surface abundance in the Philippine Sea was the
301 lowest among all of the areas (Table 1). The highest abundance of *Trichodesmium* spp.
302 (>20000 filaments L^{-1}) was observed near the Miyako Islands at St. T0906, where
303 they bloomed (see below). Tuft-shaped colonies were found at Sts. T0706, T0723,
304 CK-10, and T0906. The nitrogen fixation rate was highest in the upper 25% light
305 depth, and decreased with increasing depth at all of the stations (Fig. 3e–h). The
306 surface rates were positively correlated with the depth-integrated rates ($p < 0.05$,

307 *t*-test) (Fig. 6b), suggesting that the distribution of nitrogen fixation was indexed by
308 the surface activity. Surface and depth-integrated nitrogen fixation ranged from 0.54
309 to 62 nmol N L^{-1} d^{-1} and from 29.5 to 753 μmol N m^{-2} d^{-1}, respectively (Fig. 2d and
310 Table S1). Surface nitrogen fixation in the Philippine Sea was significantly lower than
311 that in the Kuroshio ($p < 0.05$, *t*-test).

312 The surface abundance of *Trichodesmium* spp. in the entire study area was
313 positively correlated with the nitrogen fixation rate at the surface ($r^2 = 0.80$; $p < 0.05$
314 [$r^2 = 0.55$; $p < 0.05$ if the datum taken at the *Trichodesmium*-bloom station T0906 is
315 excluded]) (Fig. 6c), suggesting that they significantly contributed to nitrogen fixation
316 in the study region. However, active nitrogen fixation occurred in the ECS where
317 *Trichodesmium* abundance was low, and hence, the other diazotrophs could also be
318 important for nitrogen fixation.

319

320 ### 3.3. **Observation around the Miyako Islands during the KT-09-17 cruise**

321 The SST was lower to the northwest of the Miyako Islands than in adjacent
322 waters, and chl *a* was enriched in the same location (Fig. 4b,c). Therefore, the
323 enhanced productivity was probably due to nutrient supply by upwelling. This
324 upwelling generally occurs in the lee of islands (Hasegawa et al., 2009), suggesting

325 that there was a northward current during the cruise. The surface salinity was lower
326 east of the Miyako Islands than in the surrounding waters (Fig. 4a). The absence of
327 any large river on the east side of Miyako-jima Island and the separation of low
328 salinity water from the island suggest that the low salinity was caused by rainfall.
329 St. T0904 was located near the upwelling water; its SST of 29.0°C was lowest and its
330 surface N+N concentration of 374 nM was highest among all of the stations. However,
331 the N+N concentration at St. T0904 at the surface was higher than that at the
332 subsurface (an approximate depth of 50 m; Fig. S4), indicating that St. T0904 was not
333 located in the middle of the upwelling. At St. T0904, the surface phosphate
334 concentration was also highest (23 nM) and the N/P ratio (=16.3) was higher than the
335 Redfield ratio. With the exception of the surface at St. T0904, the phosphate
336 concentration was low (<3–9 nM) in the upper 50 m, with no noticeable variation
337 among the stations (Fig. 2a). The dissolved iron concentration varied between 0.19
338 and 0.89 nM at the surface (Fig. 2b). The highest dissolved iron concentration was
339 observed at St. T0907.
340 During the same cruise, we encountered a *Trichodesmium* spp.-bloom at St.
341 T0906 (Fig. 2c), which had colored water at the surface. The abundance of
342 *Trichodesmium* spp. at St. T0906 was >20,000 filaments L^{-1}, which was far higher

than that at other stations (2–102 filament L^{-1}). The nitrogen fixation rate at the surface (61.9 nmol N L^{-1} d^{-1}) of this station was more than 30-fold that just below the surface, and was the highest among all of the stations (Fig. 3h). The diatom abundance was markedly higher at St. T0904 than that at the other stations. *Cylindrotheca closterium* was the most numerically dominant diatom (59%), followed by *Navicula* spp. (23%) and *Nitzschia* spp. (13%). *C. closterium* was not detected at the other stations, indicating that the high chl *a* induced by the island wake effect mainly consisted of diatoms.

3.4. **Numerical simulation**

As the Kuroshio generally flows along the continental slope north of the Miyako Islands (Fig. 1b), particles around the Miyako Islands were not transported along the typical path of the Kuroshio to the northeast, especially at their initial stages (Fig. 7a). Some particles migrated around the Miyako Islands, or turned south after they passed the Tokara Strait. Nevertheless, the particles delivered to Area K east of the Tokara Strait increased as time elapsed, and the ratio of particles delivered to Area K to the total released particles ranged from 13–56% (30 ± 16%) by day 120 in 2003–2009 (Fig. 7b). The year-to-year variations in the ratio are mainly due to influences of

361 mesoscale eddies as partly seen in the particle trajectories in Fig. 7a, and likely
362 occurred over relatively short time scales (shorter than the seasonal time scale). This
363 is supported by another series of experiments in which particles were released on June
364 1, 11, and 21, and July 1 in 2009, which yielded ratios of 6.2–38% (22 ± 13%) by day
365 120 (Fig. S5).
366

367 ## 4. DISCUSSION

368 ### 4.1. Distribution of phosphate and dissolved iron concentrations

369 Phosphate concentrations were consistently low within the MLD in all of the
370 studied areas, and the maximum abundance of *Trichodesmium* spp. and total nitrogen
371 fixation activity generally occurred near the surface, suggesting that the phosphate
372 conditions for surface *Trichodesmium* spp. and other diazotrophs were similar among
373 all of the areas. Furthermore, with the exception of St. T1004 located near the
374 continental shelf, the vertical distribution of phosphate in the Kuroshio was analogous
375 to that in the Philippine Sea. Therefore, at least in the oceanic region of the two areas,
376 phosphate availability for *Trichodesmium* spp. and the other diazotrophs was similar
377 throughout the water column.

378 The surface distribution of the dissolved iron concentration demonstrated no

379 significant variation among the areas. The dissolved iron concentration (0.19–0.89
380 nM) was higher than that in the western North Pacific subtropical region (0.15–0.4
381 nM) (Brown et al., 2005). Obata et al. (1997) demonstrated that the vertical
382 distribution of the dissolved iron concentration in the ECS showed two peaks (at the
383 surface and in the deep water), suggesting that aerial dust significantly contributes to
384 the high dissolved iron concentration at the surface in all of our study areas. In
385 accordance with our results, previous modeling studies estimated the amount of dust
386 deposition to be similar in all four areas (Jickells et al., 2005; Mahowald et al., 2009).
387 Therefore, iron availability for *Trichodesmium* spp. and the other diazotrophs was
388 also likely similar across all of the study areas. Iron can be supplied from deep water
389 to the surface by mixing processes (Johnson et al., 1999). However, if this were the
390 case, the nitrate concentration would be expected to increase simultaneously at the
391 surface (Johnson et al., 1999), and we observed no noticeable elevation in N+N in any
392 of the areas, except at St. T0904. High concentrations of dissolved iron (>0.8 nM)
393 corresponded with low salinity at Sts. T0622 and T0907, suggesting that wet
394 deposition was an important process for iron supply. Dry deposition could also be
395 important since the iron-enriched water at Sts. T0601 and T0715 did not correspond
396 with low salinity.

397 Satellite data analysis indicated that there was a “pipeline” of material transport
398 from the Miyako Islands to the Kuroshio, and this was supported by numerical
399 simulations. According to the hypothesis of Marumo and Asaoka (1974), the growth
400 of *Trichodesmium* in the Kuroshio could be maintained by the supply of iron and
401 phosphorus from the islands situated along the Kuroshio, and the Miyako Islands
402 were considered a possible nutrient source to the Kuroshio. Hence, assuming this
403 hypothesis to be valid, the iron and phosphate concentrations near the Miyako Islands
404 (especially in our observed area) would be expected to be higher than those in the
405 other areas. However, we observed no significant difference in the iron and phosphate
406 concentrations among the four areas. This suggested that there was no detectable
407 washout of iron and phosphorus from the Miyako Islands during our observations, or
408 that diazotrophs and other phytoplankton exhausted the nutrient supply close to the
409 islands.
410
411 ### *4.2.* Factors controlling the distributions of *Trichodesmium* spp. and
412 nitrogen fixation
413 Although there was no statistically significant difference in *Trichodesmium* spp.
414 abundance among the study areas probably because the data were limited and the

415 variation was large, *Trichodesmium* spp. were always observed in the Kuroshio and
416 were abundant at most stations. Furthermore, at St.CK-10 in the East China Sea which
417 is in the Kuroshio branch current, a high abundance of *Trichodesmium* spp. was
418 observed. On the other hand, *Trichodesmium* spp. abundance in the Philippine Sea
419 tended to be lower than in the other areas. Such *Trichodesmium* distribution was also
420 reported in the previous study (Marumo and Asaoka, 1974). The present study also
421 showed lower surface nitrogen fixation in the Philippine Sea compared to that in the
422 Kuroshio ($p < 0.05$, *t*-test). Previous studies demonstrated that *Trichodesmium* spp.
423 flourished in some regions of the subtropical ocean where the iron levels were high
424 (Moore et al., 2009; Shiozaki et al., 2014b), which can be attributed to the high iron
425 requirement of *Trichodesmium* spp. for their growth compared to other diazotrophs
426 and non-diazotrophs (Kustka et al., 2003; Saito et al., 2011). Therefore, the
427 distribution of *Trichodesmium* spp. in the study area was expected to be associated
428 with the dissolved iron concentration at the surface. Furthermore, the iron-enhanced
429 active nitrogen fixation causes phosphorus depletion, and is consequently limited by
430 phosphorus (Mather et al., 2008). No significant differences in surface iron and
431 phosphate were observed among the study areas, which cannot explain the
432 distribution of *Trichodesmium* spp. and nitrogen fixation in the study region.

433 Johnson et al. (1999) reported that the iron supply increased around the
434 continental shelf because re-suspension from the bottom to the euphotic zone
435 becomes significant. However, in the continental shelf of the ECS, the abundance of
436 *Trichodesmium* spp. and nitrogen fixation were low (Marumo and Asaoka, 1974;
437 Zhang et al., 2012). Zhang et al. (2012) suggested that the low nitrogen fixation in the
438 continental shelf was attributable to mixing processes and the influence of the
439 Changjiang River. Turbulence near the sea floor influences the surface water in the
440 shallower bottom region (Matsuno et al., 2006), and Zhang et al. (2012) suggested
441 that the physical disturbance reduces diazotrophy since diazotrophs including
442 *Trichodesmium* favor calm seas. Furthermore, the water in the continental shelf of the
443 ECS is strongly influenced by the Changjiang River. The N/P ratio of the Changjiang
444 River plume is significantly higher than the Redfield ratio, which results in
445 phosphorus limitation, and can contribute to the low nitrogen fixation (Zhang et al.,
446 2012). In the present study, despite the fact that the surface phosphate concentration
447 was low throughout the study areas, the N/P ratio was generally lower than the
448 Redfield ratio, suggesting that biological production was limited by the availability of
449 nitrogen compared to phosphate (Moore et al., 2008, 2013). Furthermore, the
450 insignificant difference in MLD among the ECS, the Kuroshio, and the Philippine Sea

451 (p>0.05; Tukey HSD test) indicated similar vertical mixing conditions. Therefore, the
452 environmental variables related to nitrogen fixation only slightly differed as
453 demonstrated by the nMDS plot..

454 In our study, we found a *Trichodesmium* spp. bloom near the Miyako Islands.
455 Recent studies demonstrated that *Trichodesmium* spp. thrived near oceanic islands
456 (Shiozaki et al., 2010, 2014c; Dupouy et al., 2011). Given that some aspect of the
457 environment around the islands increases *Trichodesmium* spp. abundance and that
458 they are transported from the islands to the Kuroshio, this can explain why the
459 *Trichodesmium* distribution was not estimated from environmental variables.
460 Accordingly, the low abundance of *Trichodesmium* spp. in the Philippine Sea was
461 likely due to the low density of islands. Furthermore, higher nitrogen fixation in the
462 Kuroshio than in the Philippine Sea might be explained in the same manner.
463 *Trichodesmium* is a major nitrogen fixer in the Kuroshio (Chen et al., 2008, 2014;
464 Shiozaki et al., 2014a), and our results showed that the bulk water nitrogen fixation
465 was positively correlated with *Trichodesmium* abundance.

466 The numerical simulation demonstrated that released particles from the Miyako
467 Islands were generally transported to the northeast and flowed along the Kuroshio
468 during summer between 2003 and 2009. Thus, if *Trichodesmium* increases and active

469 nitrogen fixation usually occurs around the Miyako Islands, the water would be
470 delivered to the Kuroshio. Furthermore, we performed additional particle tracking
471 experiments whose particle release points were set at major islands in the Ryukyu
472 Islands (Amami Islands, Okinawa Main Island, and the Ishigaki Islands) (Figs. S6 and
473 S7). The results demonstrated that the particles released from the other islands of the
474 Miyako Islands were also delivered to the Kuroshio, with some exceptions. Based on
475 the calculations for 2003–2009, 13–56% (30 ± 16%) of particles released from the
476 islands reached Area K by day 120 (Fig. S7).

477 Studies on nitrogen fixation around islands in the study region are fairly limited
478 (Liu et al., 2013), and the present study is the first report of a *Trichodesmium* bloom
479 around islands in the area. The Miyako Islands are surrounded by reefs, and studies
480 have shown that *Trichodesmium* blooms can be associated with reef environments
481 (Bell et al., 1999; McKinna et al., 2011). However, the factors causing the
482 *Trichodesmium* blooms around islands are not well understood (Shiozaki et al.,
483 2014c). Further studies are required to identify which characteristics of the near island
484 environment are important for the growth and/or accumulation of *Trichodesmium* and
485 other diazotrophs.

486

5. CONCLUSIONS

We hypothesize that the high abundance of *Trichodesmium* spp. and active nitrogen fixation in the Kuroshio were ascribable not to the unique nutrient environment, but rather to the supply of *Trichodesmium* spp. and other diazotrophs from the surrounding islands. The Ryukyu Islands would not be the only islands with abundant *Trichodesmium* spp., as *Trichodesmium* spp. also flourish in the upstream Kuroshio near Luzon Island (Chen et al., 2008). Therefore, the abundance of *Trichodesmium* spp. would be generally increased around islands situated along the Kuroshio, and the abundant *Trichodesmium* spp. would likely be transported to the mainstream of the Kuroshio. *Trichodesmium* is a major diazotroph in the Kuroshio (Chen et al., 2008, 2014; Shiozaki et al., 2014a), and diazotrophy in the Kuroshio is considered to influence the nutrient stoichiometry in the North Pacific (Shiozaki et al., 2010). Thus, our results indicate that phenomena around the islands located along the Kuroshio are important for determining the partial nitrogen inventory in the North Pacific.

Author Contributions

T.S., S.T., S.I., and K.F. designed the experiment and T.S., S.T., T.K., X.L., F.H., and K.F. collected the samples at sea. T.S. determined nitrogen fixation and abundance of *Trichodesmium* spp. during the KT-06-21, KT-07-21, KT-09-17, and *Nagasaki-maru* 242 cruises, and X.L. did during the KT-10-19 cruise. T.S. analyzed datasets of satellite and climatological current field. S.T. analyzed concentration of dissolved iron. S.I. performed numerical experiments. T.K. and F.H. determined nutrient concentration. T.S. prepared the manuscript with contributions from all co-authors.

Acknowledgements

We thank J. Ishizaka, the captains, crew members, and participants on board the T/V *Nagasaki-maru* and R/V *Tansei-maru* cruises for their cooperation at sea. Thanks also to K. Hayashizaki for his support in use of the mass spectrometer at Kitasato University, to A. Takeshige and J. Hirai for their valuable comments on biology in the Kuroshio, and to T. Kitahashi for his suggestion on statistical analyses. We appreciate NASA ocean color processing group for providing the chl *a* data set and Japan Oceanographic Data Center for ADCP data set. This research was financially supported by MEXT grant on Priority Areas (18067006 & 21014006) and

521 by Innovative Areas (24121001, 24121005, & 24121006) and by Grant-in-Aid for
522 JSPS Fellows (25-7341).
523

524 **References**

525 Bell, P.R.F., Elmetri, I., Uwins, P.: Nitrogen fixation by *Trichodesmium* spp. in the
526 central and northern Great Barrier Reef lagoon: relative importance of the
527 fixed-nitrogen load, Mar. Ecol. Progr. Ser., 186, 119-126, 1999.

528 Brown, M.T., Landing, W.M., Measures, C.I.: Dissolved and particulate Fe in the
529 western and central North Pacific: Results from the 2002 IOC cruise, Geochem.
530 Geophys. Geosyst., 6(10), Q10001, 2005.

531 Capone, D.G., Zehr, P.J., Paerl, H.W., Bergman, B., Carpenter, E.J.: *Trichodesmium*,
532 a globally significant marine cyanobacterium, Science, 276, 1221-1229, 1997.

533 Chen, C.T.A.: Distributions of nutrients in the East China Sea and the South China
534 Sea connection, J. Oceanogr., 64, 737-751, 2008.

535 Chen, Y.L.L., Chen, H.Y., Tuo, S.H., Ohki, K.: Seasonal dynamics of new production
536 from *Trichodesmium* N_2 fixation and nitrate uptake in the upstream Kuroshio and
537 South China Sea basin, Limnol. Oceanogr., 53(5), 1705-1721, 2008.

538 Chen, Y.L.L., Chen, H.Y., Lin, Y.H., Yong, T.C., Taniuchi, Y., Tuo, S.H.: The
539 relative contributions of unicellular and filamentous diazotrophs to N_2 fixation in the
540 South China Sea and the upstream Kuroshio, Deep-Sea Res. I, 85, 56-71, 2014.

541 Dabundo, R., Lehmann, M.F., Treibergs, L., Tobias, C.R., Altabet, M.A.: The

542 contamination of commercial $^{15}N_2$ gas stocks with ^{15}N-labeled nitrate and ammonium
543 and consequences for nitrogen fixation measurements, PLoS one, 9(10), e110335,
544 2014.
545 Dupouy, C., Benielli-Gary, D., Neveux, J., Dandonneau, Y., Westberry, T.K.: An
546 algorithm for detecting *Trichodesmium* surface blooms in the South Western Tropical
547 Pacific, Biogeosciences, 8, 3631-3647, 2011.
548 Großkopf, T., Mohr, W., Baustian, T., Schunck, H., Gill, D., Kuypers, M.M.M., Lavik,
549 G., Schmitz, R.A., Wallace, D.W.R., LaRoche, J.: Doubling of marine
550 dinitrogen-fixation rate based on direct measurements, Nature, 488, 361-364, 2012.
551 Hasegawa, D., Lewis, M.R., Gangopadhyay, A.: How islands cause phytoplankton to
552 bloom in their wake, Geophys. Res. Lett., 36, L20605, 2009.
553 Hashihama, F., Furuya, K., Kitajima, S., Takeda, S., Takemura, T., Kanda, J.:
554 Macro-scale exhaustion of surface phosphate by dinitrogen fixation in the western
555 North Pacific, Geophys. Res. Lett., 36, L03610, 2009.
556 Isobe, A.: Recent advances in ocean-circulation research on the Yellow Sea and East
557 China Sea shelves, J. Oceanogr., 64, 569-584, 2008.
558 Itoh, S., Yasuda, I., Nishikawa, H., Sasaki, H., Sasai, Y.: Transport and environmental
559 temperature variability of eggs and larvae of the Japanese anchovy (*Engraulis*

560 *japonicus*) and Japanese sardine (*Sardinops melanostictus*) in the western North
561 Pacific estimated via numerical particle-tracking experiments, Fish. Oceanogr., 18(2),
562 118-133, 2009.Jickells, T.D., An, Z.S., Andersen, K.K., Baker, A.R., Bergametti, G.,
563 Brooks, N., Cao, J.J., Boyd, P.W., Duce, R.A., Hunter, K.A., Kawahata, H., Kubilay,
564 N., LaRoche, J., Liss, P.S., Mahowald, N., Prospero, J.M., Ridgwell, A.J., Tegen, I.,
565 Torres, R.: Global iron connections between desert dust, ocean biogeochemistry, and
566 climate, Science, 308, 67-71, 2005.
567 Johnson, K.S., Chavez, F.P., Friederich, G.E.: Continental-shelf sediment as a
568 primary source of iron for coastal phytoplankton, Nature, 398, 697-700, 1999.
569 Johnson, K.S., Boyle, E., Bruland, K., Coale, K., Measures, C., Moffett, J.,
570 Aguilar-Islas, A., Barbeau, K., Bergquist, B., Bowie, A., Buck, K., Cai, Y., Chase, Z.,
571 Cullen, J., Doi, T., Elrod, V., Fitzwater, S., Gordon, M., King, A., Laan, P.,
572 Laglera-Baquer, L., Landing, W., Lohan, M., Mendez, J., Milne, A., Obata, H.,
573 Ossiander, L., Plant, J., Sarthou, G., Sedwick, P., Smith, G.J., Sohst, B., Tanner, S.,
574 Van den Berg, S., Wu, J.: The SAFe iron intercomparison cruise: an international
575 collaboration to develop dissolved iron in seawater standards, Eos, 88, 131-132, 2007.
576 Kodama, T., Furuya, K., Hashihama, F., Takeda, S., Kanda, J.: Occurrence of
577 rain-origin nitrate patches at the nutrient-depleted surface in the East China Sea and

578 the Philippine Sea during summer, J. Geophys. Res., 116, C08003, 2011.

579 Kustka, A., Sañudo-Wilhelmy, S., Carpenter, E.J., Capone, D.G., Raven, J.A.: A

580 revised estimate of the iron use efficiency of nitrogen fixation, with special reference

581 to the marine cyanobacterium *Trichodesmium* spp. (Cyanophyta), J. Phycol., 39,

582 12-25, 2003.

583 Liu, X., Furuya, K., Shiozaki, T., Masuda, T., Kodama, T., Sato, M., Kaneko, H.,

584 Nagasawa, M., Yasuda, I.: Variability in nitrogen sources for new production in the

585 vicinity of the shelf edge of the East China Sea in summer, Cont. Shelf Res., 61-62,

586 23-30, 2013.

587 McKinna, L.I.W., Furnas, M.J., Ridd, P.V.: A simple, binary classification algorithm

588 for detection of *Trichodesmium* spp. within the Great Barrier Reef using MODIS

589 imagery, Limnol. Oceanogr.; Methods, 9, 50-66, 2011.

590 Mahaffey, C., Michaels, A.F., Capone, D.G.: The conundrum of marine N_2 fixation,

591 Am. J. Sci., 305, 546-595, 2005.

592 Mahowald, N.M., Engelstaedter, S., Luo, C., Sealy, A., Artaxo, P., Benitez-Nelson, C.,

593 Bonnet, S., Chen, Y., Chuang, P.Y., Cohen, D.D., Dulac, F., Herut, B., Johansen,

594 A.M., Kubilay, N., Losno, R., Maenhaut, W., Paytan, A., Prospero, J.M., Shank, L.M.,

595 Siefert, R.L.: Atmospheric iron deposition: Global distribution, variability, and human

perturbations, Annu. Rev. Mar. Sci., 1, 245-278, 2009.

Marumo, R., Asaoka, O.: *Trichodesmium* in the East China Sea 1. Distribution of *Trichodesmium thiebautii* GOMONT during 1961-1967, J. Oceanogr. Soc. Japan, 30, 298-303, 1974.

Mather, R.L., Reynolds, S.E., Wolff, G.A., Williams, R.G., Torres-Valdes, S., Woodward, E.M.S., Landolfi, A., Pan, X., Sanders, R., Achterberg, E.P.: Phosphorus cycling in the North and South Atlantic Ocean subtropical gyres, Nat. Geosci., 1, 439-443, 2008.

Matsuno, T., Lee, J.S., Shimizu, M., Kim, S.H., Pang, I.C.: Measurements of the turbulent energy dissipation rate ε and an evaluation of the dispersion process of the Changjiang Diluted Water in the East China Sea, J. Geophys. Res., 111, C11S09, 2006.

McGowan, J.A.: Oceanic biogeography of the Pacific, in: The microplaleontology of the oceans, Cambridge University Press, Cambridge, 3-74, 1971.

Miyazawa, Y., Zhang, R., Guo, X., Tamura, H., Ambe, D., Lee, J.S., Okuno, A., Yoshinari, H., Setou, T., Komatsu, K.: Water mass variability in the western North Pacific detected in a 15-year eddy resolving ocean reanalysis, J. Oceanogr., 65, 737-756, 2009.

614 Mohr, W., Großkopf, T., Wallace, D.W.R., LaRoche, J.: Methodological
615 underestimation of oceanic nitrogen fixation rate, PLoS one, 5(9), e12583, 2010.
616 Montoya, J.P., Voss, M., Kähler, P., Capone, D.G.: A simple, high-precision,
617 high-sensitivity tracer assay for N_2 fixation, Appl. Environ. Microbiol., 62(3),
618 986-993, 1996.
619 Moore, C.M., Mills, M.M., Langlois, R., Milne, A., Achterberg, E.P., LaRoche, J.,
620 Geider, R.J.: Relative influence of nitrogen and phosphorus availability on
621 phytoplankton physiology and productivity in the oligotrophic sub-tropical North
622 Atlantic Ocean, Limnol. Oceanogr., 53(1), 291-305, 2008.
623 Moore, C.M., Mills, M.M., Achterberg, E.P., Geider, R.J., LaRoche, J., Lucas, M.I.,
624 McDonagh, E.L., Pan, X., Poulton, A.J., Rijkenberg, M.J.A., Suggett, D.J., Ussher,
625 S.J., Woodward, E.M.S.: Large-scale distribution of Atlantic nitrogen fixation
626 controlled by iron availability, Nat. Geosci., 2, 867-871, 2009.
627 Moore, C.M., Mills, M.M., Arrigo, K.R., Berman-Frank, I., Bopp, L., Boyd, P.W.,
628 Galbraith, E.D., Geider, R.J., Guieu, C., Jaccard, S.L., Jickells, T.D., LaRoche, J.,
629 Lenton, T.M., Mahowald, N.M., Marañon, E., Marinov, I., Moore, J.K., Nakatsuka, T.,
630 Oschlies, A., Saito, M.A., Thingstad, T.F., Tsuda, A., Ulloa, O.: Processes and
631 patterns of oceanic nutrient limitation, Nat. Geosci., 6, 701-710, 2013.

632 Obata, H., Karatani, H., Nakayama, E.: Automated determination of iron in seawater
633 by chelating resin concentration and chemiluminescence detection, Anal. Chem., 65,
634 1524-1528, 1993.
635 Obata, H., Karatani, H., Matsui, M., Nakayama, E.: Fundamental studies for chemical
636 speciation of iron in seawater with an improved analytical method, Mar. Chem., 56,
637 97-106, 1997.
638 Saito, M.A., Bertrand, E.M., Dutkiewicz, S., Bulygin, V.V., Moran, D.M., Monteiro,
639 F.M., Follows, M.J., Valois, F.W., Waterbury, J.B.: Iron conservation by reduction of
640 metalloenzyme inventories in the marine diazotroph *Crocosphaera watsonii*, Proc.
641 Natl. Acad. Sci. USA, 108, 2184-2189, 2011.
642 Shiozaki, T., Furuya, K., Kodama, T., Takeda, S.: Contribution of N_2 fixation to new
643 production in the western North Pacific Ocean along 155ºE, Mar. Ecol. Progr. Ser.,
644 377, 19-32, 2009.
645 Shiozaki, T., Furuya, K., Kodama, T., Kitajima, S., Takeda, S., Takemura, T., Kanda,
646 J.: New estimation of N_2 fixation in the western and central Pacific Ocean and its
647 marginal seas,. Glob. Biogeochem. Cycles, 24, GB1015, 2010.
648 Shiozaki, T., Furuya, K., Kurotori, H., Kodama, T., Takeda, S., Endoh, T., Yoshikawa,
649 Y., Ishizaka, J., Matsuno, T.: Imbalance between vertical nitrate flux and nitrate

650 assimilation on a continental shelf: Implications of nitrification, J. Geophys. Res., 116,
651 C10031, 2011.
652 Shiozaki, T., Chen, Y.L.L., Lin, Y.H., Taniuchi, Y., Sheu, D.S., Furuya, K., Chen,
653 H.Y.: Seasonal variations of unicellular diazotroph groups A and B, and
654 *Trichodesmium* in the northern South China Sea and neighboring upstream Kuroshio
655 Current, Cont. Shelf Res., 80, 20-31, 2014a.
656 Shiozaki, T., Ijichi, M., Kodama, T., Takeda, S., Furuya, K.: Heterotrophic bacteria as
657 major nitrogen fixers in the euphotic zone of the Indian Ocean, Glob. Biogeochem.
658 Cycles, 28, 1096-1110, 2014b.
659 Shiozaki, T., Kodama, T., Furuya, K.: Large-scale impact of the island mass effect
660 through nitrogen fixation in the western South Pacific Ocean, Geophys. Res. Lett., 41,
661 2907-2913, 2014c.
662 Wilson, C., Qiu, X.: Global distribution of summer chlorophyll blooms in the
663 oligotrophic gyres, Progr. Oceanogr., 78, 107-134, 2008.
664 Zhang, R., Chen, M., Cao, J., Ma, Q., Yang, J., Qiu, Y.: Nitrogen fixation in the East
665 China Sea and southern Yellow Sea during summer 2006, Mar. Ecol. Progr. Ser., 447,
666 77-86, 2012.
667

668 Table 1 Summary of *Trichodesmium* at the surface, and depth-integrated nitrogen

669 fixation and its related parameters in the four representative study areas.

Area	*Trichodesmium*[*] [filaments l^{-1}]	N_2 fixation [μmolN L^{-1} d^{-1}]	Temperature[*] [ºC]	MLD [m]	$NO_3^-+NO_2^{-*,\dagger}$ [nM]	$PO_4^{3-*,\dagger}$ [nM]	DFe[*] [nM]
East China Sea	21±58	170±140	28.5±1.2	24±12	19±11	15±9	0.76±0.18
Kuroshio	43±33	199±142	29.4±0.81	27±8	9±8	15±7	0.45±0.13
Philippine Sea	8±8	58.3±25.1	29.4±0.1	23±3	8±3	14±19	0.51±0.25
Miyako Islands	3019±8478	201±274	29.3±0.3	40±12	61±128	8±7	0.38±0.24

670 [*] values in surface water

671 [†]When the concentration was below the detection limit (3 nM), we assumed a concentration of 3 nM to

672 calculate the mean.

673

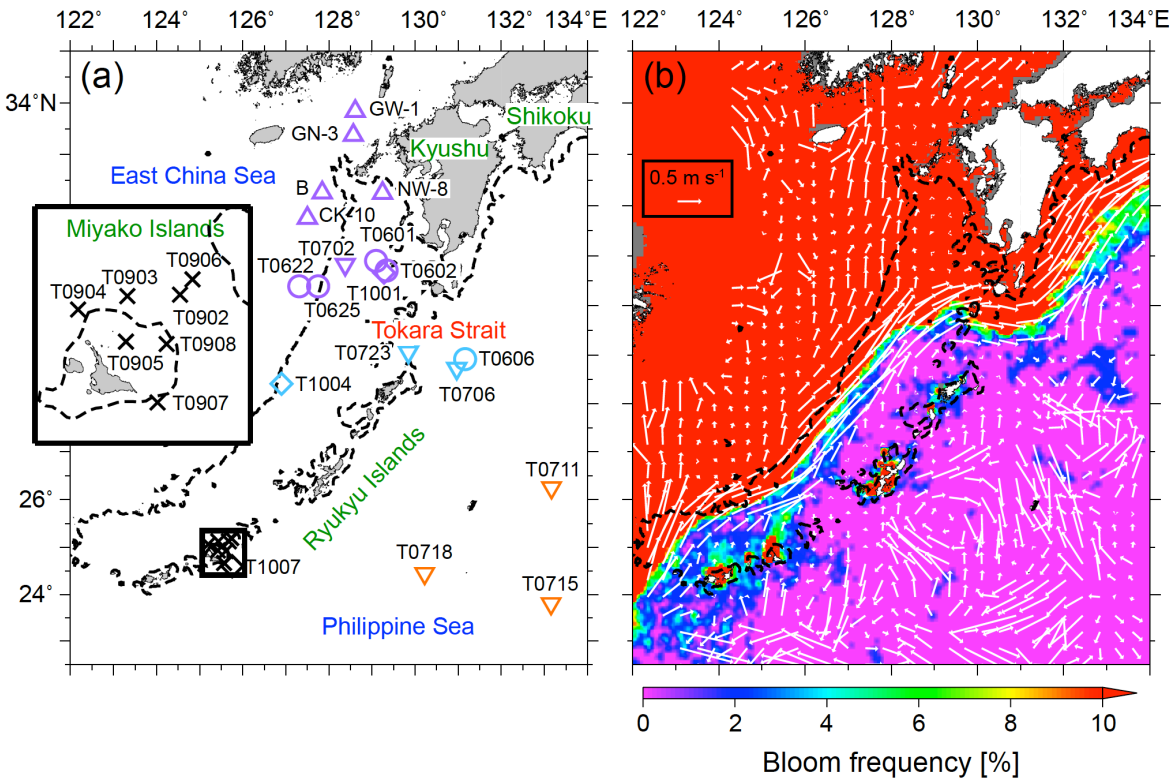

674

675

676 Figure 1. (a) Sampling stations during the KT-06-21 (circles), KT-07-22 (inverted
677 triangles), KT-09-17 (crosses), KT-10-19 (diamonds), and 242 (triangles) cruises.
678 Symbols of stations located in the East China Sea, the Kuroshio, the Philippine Sea,
679 and near the Miyako Islands are indicated in purple, light blue, orange, and black,
680 respectively. (b) Climatological surface current fields during summer (1953–2008)
681 from geoelectrokinetograph measurements and ship-mounted ADCP data. The
682 background contour represents the percentage of chlorophyll *a* of >0.15 mg m^{-3}
683 during summer between 2003 and 2009. Dashed lines indicate 200 m isobaths.

684

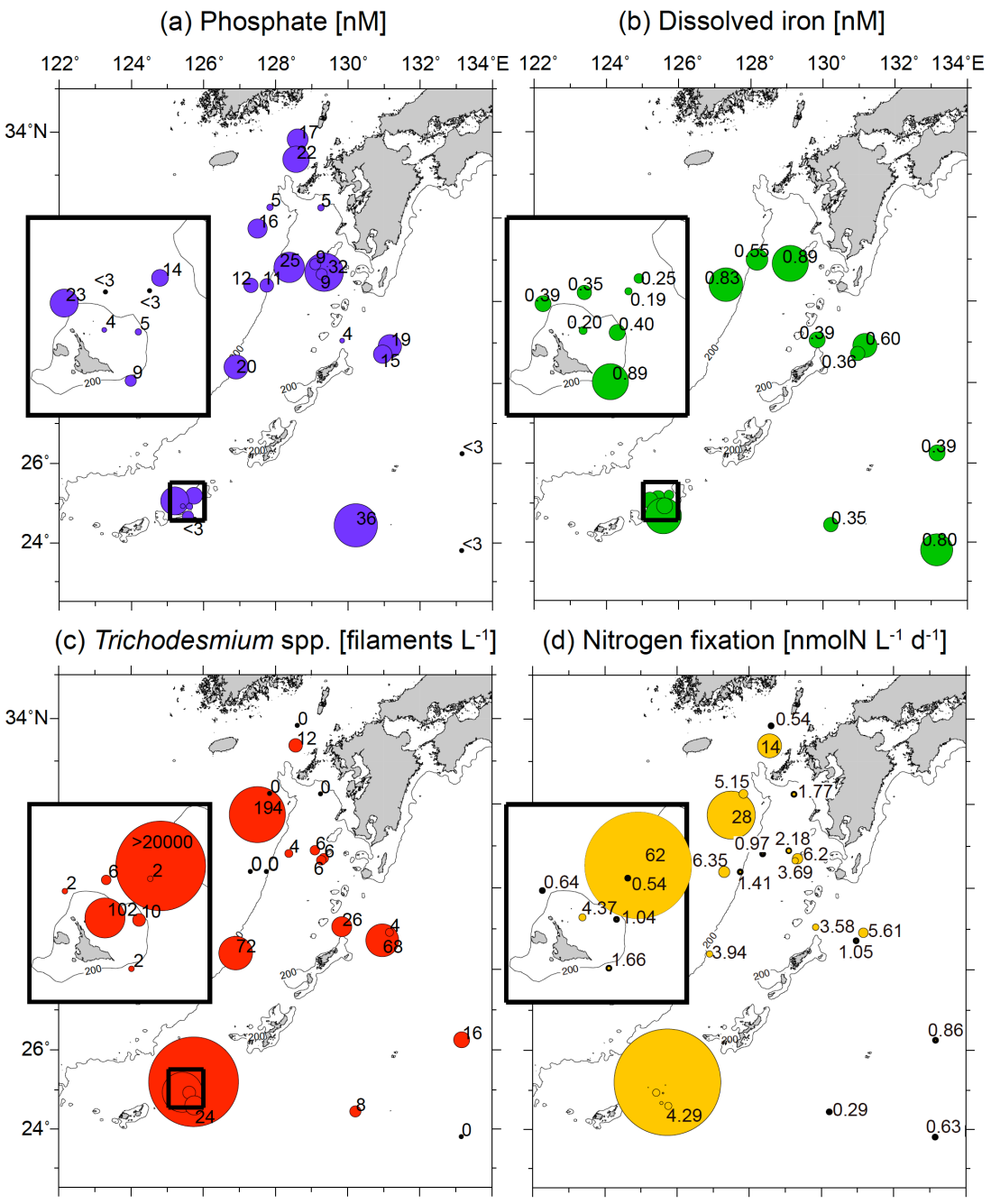

685

686

687 Figure 2. Distribution of (a) phosphate, (b) dissolved iron, (c) *Trichodesmium* spp.,

688 and (d) nitrogen fixation at the surface. The parameters in the small boxes indicate

689 results from the KT-09-17 cruise. The areas of the circles are proportional to the

690 concentration, abundance, or activity.

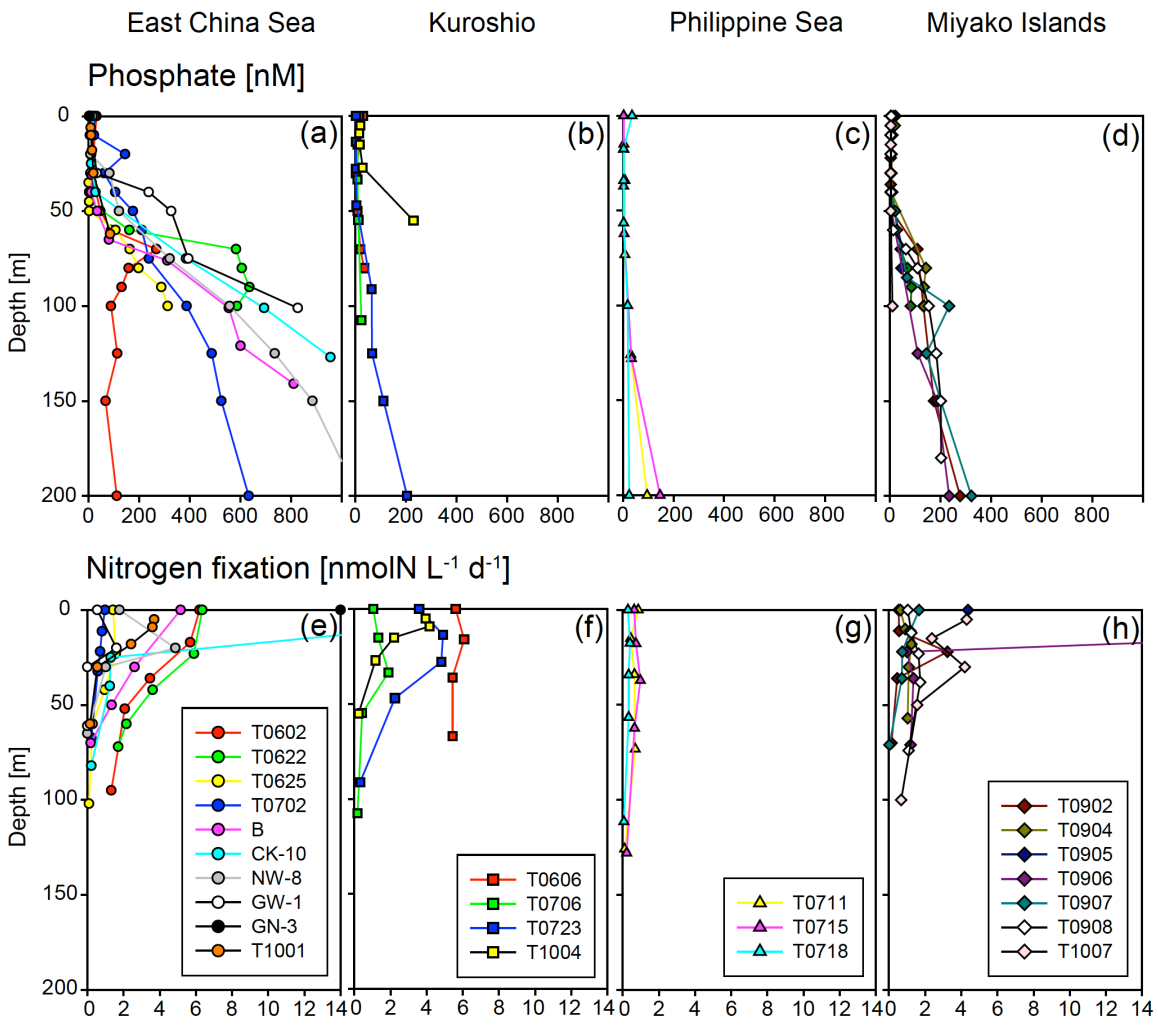

691

692

693 Figure 3. Vertical profiles of phosphate and nitrogen fixation in the East China Sea (a

694 and e), the Kuroshio (b and f), the Philippine Sea (c and g), and the Miyako Islands (d

695 and h).

696

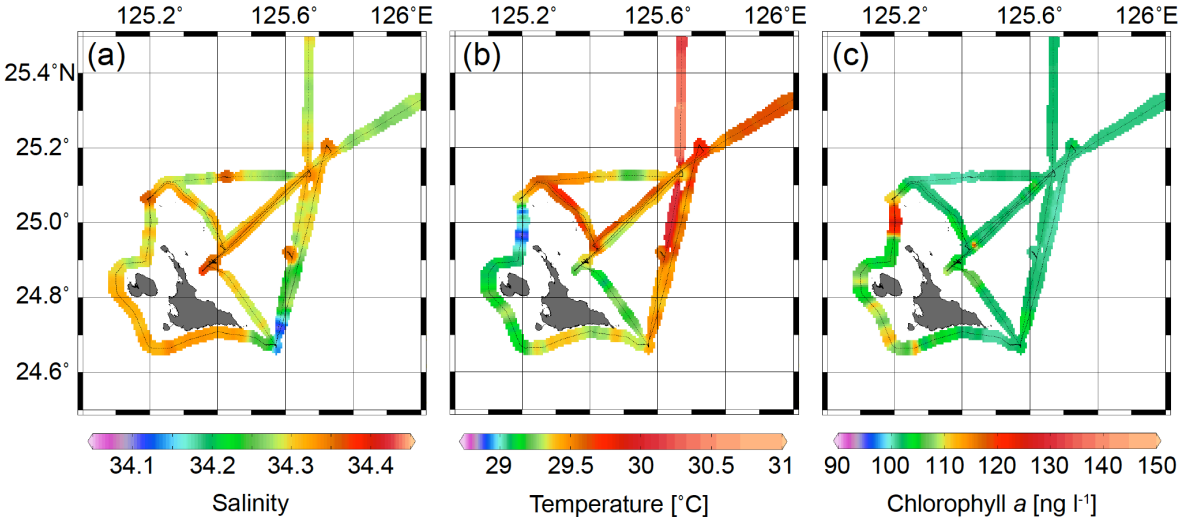

697

698

699 Figure 4. Surface (a) salinity, (b) temperature, and (c) chlorophyll *a* during the

700 KT-09-17 cruise.

701

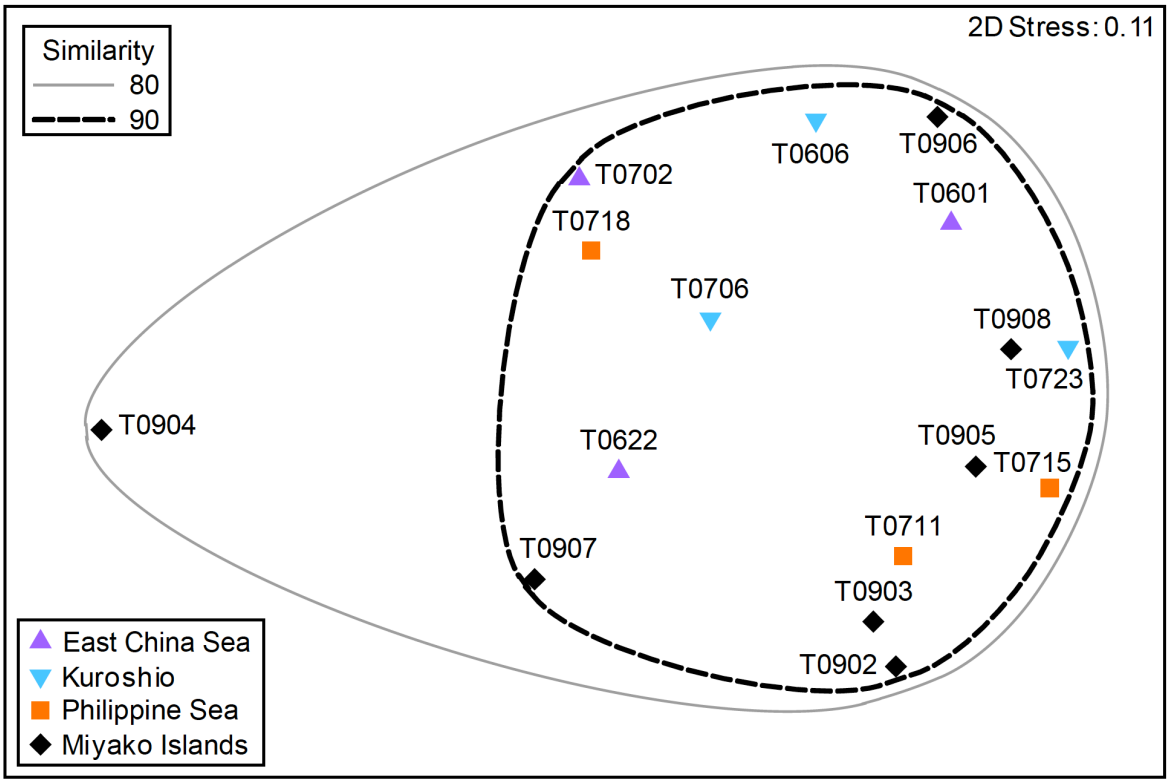

Figure 5. nMDS ordination of sampling stations with environmental variables

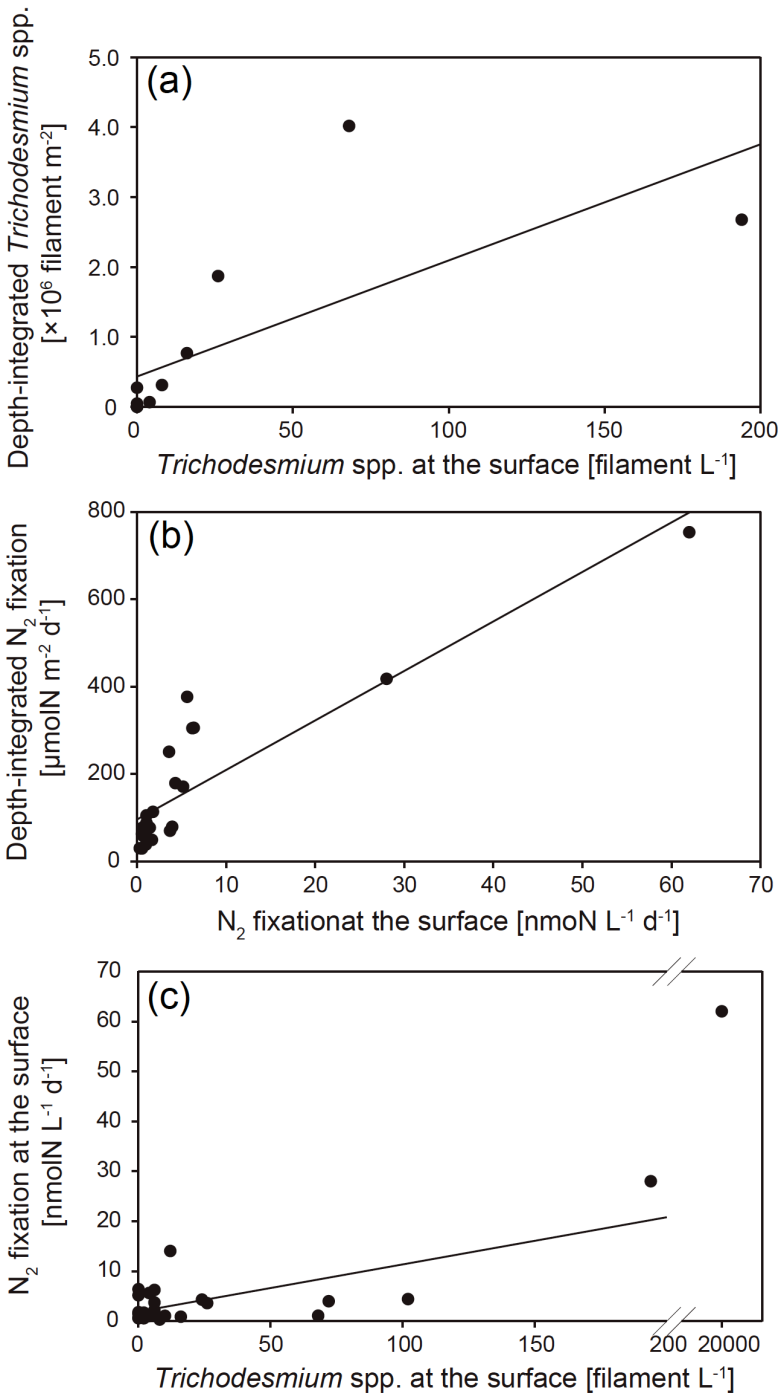

706

707

708 Figure 6. Relationships (a) between surface and depth-integrated *Trichodesmium* spp.

709 abundance, (b) between surface and depth-integrated nitrogen fixation rates, and (c)

710 between *Trichodesmium* spp. abundance and nitrogen fixation rate at the surface.

711

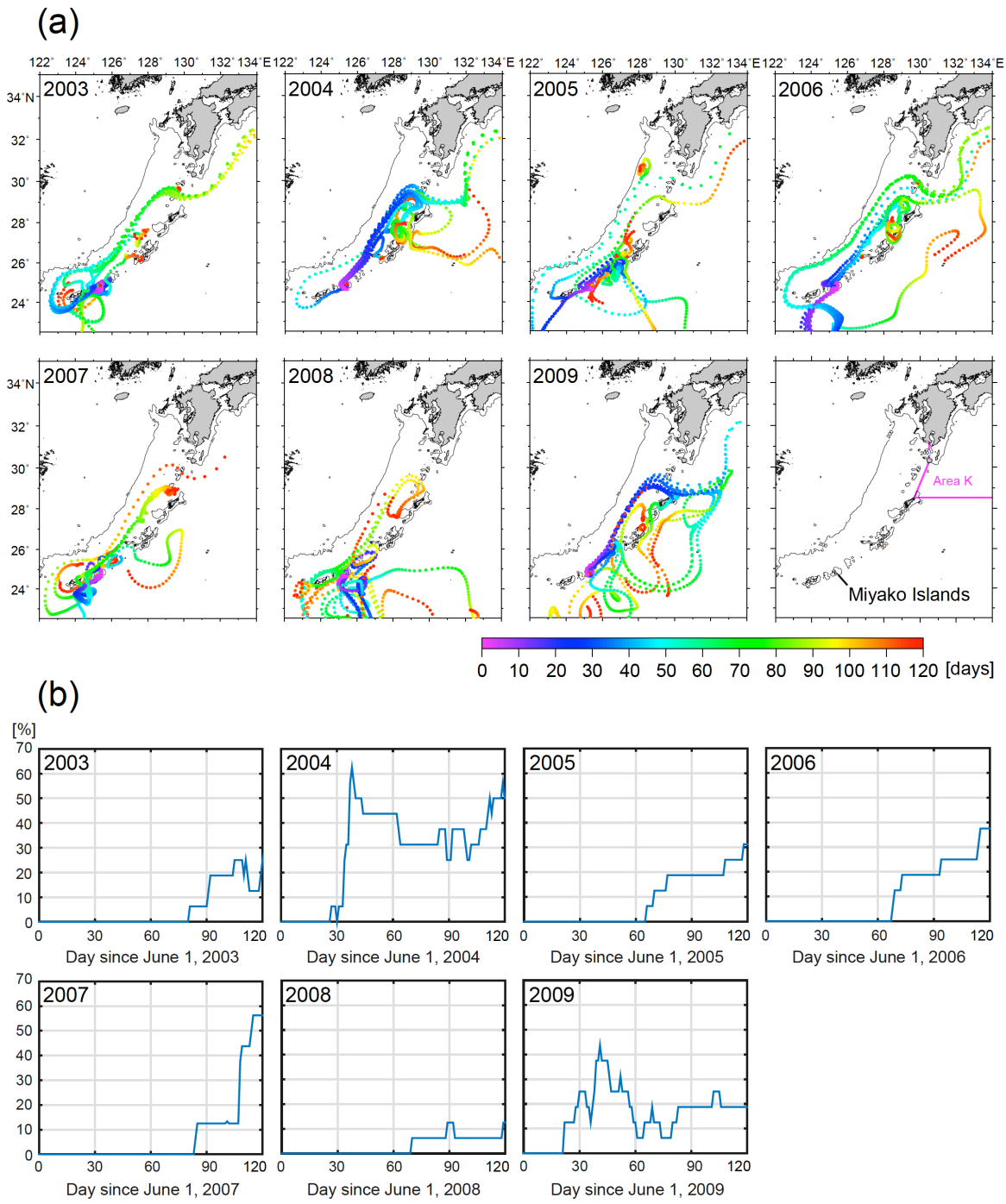

712

713

714 Figure 7. (a) Trajectories of particles released from points around the Miyako Islands

715 on June 1, 2003–2009. (b) The ratio of particles delivered to Area K to the total

716 released particles.